

Response of the Magnetosphere to Microscopic Effects in Auroral Arc Formation^{*)}

Hiroki HASEGAWA, Nobuaki OHNO¹⁾ and Tetsuya SATO¹⁾

National Institute for Fusion Science, 322-6 Oroshi-cho, Toki 509-5292, Japan

¹⁾*University of Hyogo, 7-1-28 Minatojimaminami-machi, Chuo-ku, Kobe 650-0047, Japan*

(Received 21 December 2010 / Accepted 1 August 2011)

A process of quiet auroral arc formation, in particular, the response of the magnetosphere to the effect of auroral energetic electrons, is studied using a holistic auroral simulation code. It consists of a three-dimensional magnetohydrodynamic code for a dipole magnetosphere-ionosphere coupling system and a one-dimensional electrostatic plasma particle code for auroral energetic electron production. Results of the holistic auroral simulation indicate that drastic variation in the ionospheric electric field, which is induced by auroral energetic electrons and propagates into the magnetosphere, influences the magnetospheric field-aligned current distribution. Furthermore, the characteristic time scale of this process is investigated.

© 2011 The Japan Society of Plasma Science and Nuclear Fusion Research

Keywords: aurora, magnetosphere-ionosphere coupling, feedback instability, electron acceleration, holistic simulation

DOI: 10.1585/pfr.6.2401128

1. Introduction

The macroscopic structure of a quiet auroral arc is thought to be formed by interactions between the magnetosphere and ionosphere. Ionospheric feedback instability [1] is believed to be a candidate mechanism that could explain this phenomenon. However, observations of the growth of field-aligned current density and ionospheric plasma density cannot be fully explained by macroscopic instability [2]. Ionization of ionospheric neutral particles by auroral energetic electrons may play an important role in the more intensive growth of the densities.

On the other hand, a certain type of auroral energetic electrons is believed to be produced by the super ion-acoustic double layer [3]. This layer is formed through microscopic instability, which is induced by the intensive field-aligned current enhanced through the feedback instability.

We investigated the formation of quiet auroral arcs through a holistic simulation code that consists of a three-dimensional magnetohydrodynamic (MHD) code for a dipole magnetosphere-ionosphere (M-I) coupling system and a one-dimensional electrostatic plasma particle code for auroral energetic electron production [4]. This code has been developed using the “macro-micro interlocked (MMI) algorithm” [5], which enables transferring the microscopic effect into the macroscopic phenomenon without simple macroscopic parameters.

The simultaneous and self-consistent holistic simulation revealed that the ionospheric plasma density inten-

sively increases. This is because of the ionization of ionospheric neutral particles by electrons that are accelerated by the super ion-acoustic double layer. The ionospheric electric field sharply decreases with the ionospheric plasma density growth. In this study, we show that such changes in the ionospheric plasma density influence the field-aligned current owing to the propagation of the ionospheric electric field into the magnetosphere. Furthermore, we investigate the characteristic time scale of this modification. In Sec. 2, we briefly review the auroral MMI simulation model and explain the simulation parameters. In Sec. 3, we present the result of the MMI simulation. Section 4 summarizes the paper.

2. Methodology

2.1 Auroral MMI simulation model

The auroral MMI simulation code consists of MHD (macro) and particle (micro) components. The simulation system of the macro component uses three-dimensional dipole coordinates to describe a dipole geomagnetic field. The simulation region is confined within a certain high-latitude volume enclosed by the two (high and low latitude) dipolar boundary surfaces extending from the ionosphere, at the bottom, to the equatorial magnetosphere, at the top (see Fig. 4 in Ref. [2]). The dynamics of the magnetosphere are described by the following one-fluid MHD equations:

$$\frac{\partial \mathbf{B}}{\partial t} = -\nabla \times \mathbf{E}, \quad (1)$$

$$\frac{\partial(\rho \mathbf{v})}{\partial t} = -\nabla \cdot (\rho \mathbf{v} \mathbf{v}) + \mathbf{j} \times \mathbf{B}, \quad (2)$$

$$\mathbf{E} = -\mathbf{v} \times \mathbf{B}, \quad (3)$$

author's e-mail: hasegawa.hiroki@nifs.ac.jp

^{*)} This article is based on the presentation at the 20th International Toki Conference (ITC20).

$$\mu_0 \mathbf{j} = \nabla \times \mathbf{B}, \quad (4)$$

where \mathbf{B} , \mathbf{E} , \mathbf{v} , \mathbf{j} , ρ , and μ_0 are the magnetic field, the electric field, the velocity of the plasma flow, the current density, the mass density, and the permeability, respectively. At the magnetospheric equatorial plane, a twin-vortex convection flow is given permanently as a boundary condition. This plasma convection induces the region 1 current system and the ionospheric feedback instability. At the ionospheric boundary, the following elliptic partial differential equation of the ionospheric electric potential Φ_{IS} :

$$\nabla_{\perp} \cdot \left(ehM_{\text{P}} n (\nabla_{\perp} \Phi_{\text{IS}}) + ehM_{\text{H}} \frac{\mathbf{B}_{\text{IS}} \times (\nabla_{\perp} \Phi_{\text{IS}})}{|\mathbf{B}_{\text{IS}}|} \right) = j_{\parallel}, \quad (5)$$

is solved for each time step. Here, \mathbf{B}_{IS} and n are the geomagnetic field at the ionospheric height and the ionospheric plasma number density, respectively; e is the electronic charge; h is the effective height range of the ionospheric region of interest; M_{P} and M_{H} are the Pedersen and Hall mobilities, respectively; j_{\parallel} is the field-aligned current at the ionospheric height. The subscript \perp refers to quantities or operators that are on the surface perpendicular to the geomagnetic field. In addition, the time evolution of the ionospheric plasma density is calculated by integrating the following ionospheric plasma density continuity equation:

$$\frac{\partial n}{\partial t} = \frac{(\nabla_{\perp} \Phi_{\text{IS}}) \times \mathbf{B}_{\text{IS}}}{|\mathbf{B}_{\text{IS}}|^2} \cdot \nabla_{\perp} n + \frac{j_{\parallel}}{eh} - \alpha(n^2 - n_0^2), \quad (6)$$

where α is the recombination coefficient (The details of the macro component are shown in Ref. [2]).

On the other hand, the micro component is a one-dimensional electrostatic plasma particle code. In the particle code, the full particle dynamics and the self-consistent electric field are solved. It is assumed that the initial electron velocity distribution is supplied by the shifted Maxwellian with drift velocity v_{d} and the initial ion velocity distribution is given by the Maxwellian. Furthermore, the particle code adopts an open boundary system with the constant current model, in which injected particles at boundaries of a simulation box are determined by constant current condition throughout the system [6] (A more detailed description of the particle code is presented in Ref. [7]).

The procedure of connecting the MHD and the particle components is as follows. First, in the MHD simulation for the M-I coupling system, the field-aligned current growth due to the feedback instability is calculated. Second, the ionospheric boundary is examined for isolated areas in which the field-aligned current at the ionospheric height exceeds a certain critical value ($j_{\parallel \text{c}}$). Next, maximum values of the field-aligned current in such intensive growth areas ($j_{\parallel \text{peak}}$) are transferred from the MHD (macroscopic) side to the particle (microscopic) side. Then, in the particle simulation, the electron-drift velocity v_{d} is calculated from the maximum value of the

field-aligned current. By using v_{d} as the initial condition, the electron acceleration by the ion-acoustic double layer is simulated. At the end of the particle simulation, we obtain the ionospheric plasma production rate and the auroral emission intensity from the energy spectrum of the precipitating electrons on the downstream boundary of the system. Finally, the obtained ionospheric plasma production rate is transferred to the MHD simulation and added to Eq. (6). Then, the MHD simulation is continued (The details of the connection procedure are described in Ref. [4]).

2.2 Simulation parameters

Here, we briefly describe the simulation conditions and parameters. First, the MHD simulation is described as follows. The ionospheric auroral zone (region 1 auroral oval) is from latitudes 70.0° to 72.3° . The grid numbers in the field line (ψ), the latitudinal (χ), and the longitudinal (ϕ) directions are 1279, 66, and 256, respectively. Here, we define ψ as the direction extending from the ionosphere to the magnetospheric equator along the geomagnetic field, χ as the direction toward the equator along the meridian, and ϕ as the direction toward the east along the parallel of latitude. The effective height range of the ionospheric region of interest is $h = 1.2 \times 10^4$ m. The recombination coefficient is $\alpha = 3.0 \times 10^{-13} \text{ m}^3 \text{ s}^{-1}$. The Pedersen and Hall mobilities are $M_{\text{P}} = 1.6 \times 10^4 \text{ m}^2 \text{ s}^{-1} \text{ V}^{-1}$ and $M_{\text{H}} = 3.2 \times 10^4 \text{ m}^2 \text{ s}^{-1} \text{ V}^{-1}$, respectively. The initial ionospheric plasma density is uniform as $n_0 = 3.0 \times 10^{10} \text{ m}^{-3}$. The Alfvén speed is uniform and constant as $v_{\text{A}} = 1.0 \times 10^6 \text{ m s}^{-1}$. The geomagnetic field strength at the ionosphere height is $B_{\text{IS}} = -3.1 \times 10^{-5} \text{ T}$. The earth's radius is $R_{\text{E}} = 6.37 \times 10^6 \text{ m}$. The Alfvén transit time τ_{A} , which is the time for propagation of an Alfvén wave from the magnetospheric equator to the ionosphere, is $\tau_{\text{A}} = 88.7 \text{ s}$. The time step is $\Delta t_{\text{M}} = 2.9 \times 10^{-3} \text{ s}$.

Next, the parameters for the connection between the MHD and the particle simulations are mentioned. It is assumed that the temperature of precipitating electrons is $T_{\text{e}} = 100 \text{ eV}$. The threshold of the field-aligned current is $j_{\parallel \text{c}} = 1.0 \times 10^{-6} \text{ Am}^{-2}$. If $j_{\parallel \text{peak}} = j_{\parallel \text{c}}$, the electron drift velocity is $v_{\text{d}}/v_{\text{T}_{\text{e}}} = 0.4$, which is close to the lower threshold of the ion-acoustic double layer creation [3, 7]. Here, $v_{\text{T}_{\text{e}}}$ is the electron thermal velocity.

The parameters in the particle simulation are as follows. The grid spacing is $\Delta_{\text{g}} = \lambda_{\text{D}}$, where λ_{D} is the Debye length. The total system length is $L_{\text{p}} = 1024 \lambda_{\text{D}}$. The ion-to-electron mass ratio is $m_{\text{i}}/m_{\text{e}} = 100$. The electron-to-ion temperature ratio is $T_{\text{e}}/T_{\text{i}} = 20$. There are 10,240 electrons and an equal number of ions per grid. The total number of time steps for one run is $N_{\text{t}}^{\text{p}} = 39,250$. The time step Δt_{p} is equal to or smaller than $0.16 \omega_{\text{pe}}^{-1}$ and dependent on v_{d} (Eq. (31) in Ref. [7]). Here, ω_{pe} is the plasma frequency.

Detailed descriptions of parameters and boundary conditions are shown in Refs. [2, 7].

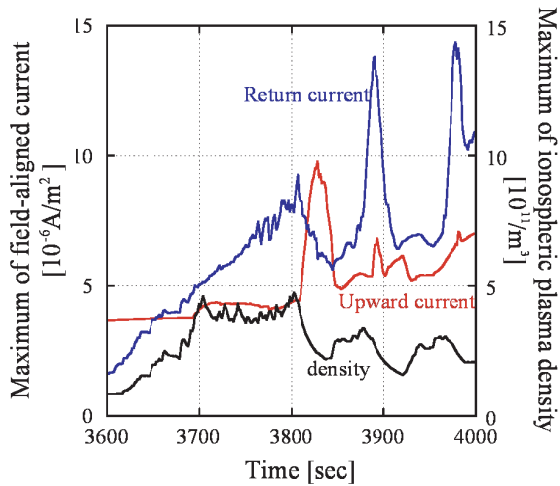


Fig. 1 Time variations in the maxima of the upward (red line) and downward (blue line) field-aligned current densities at the ionosphere height and the ionospheric plasma density (black line).

3. Simulation Results

Figure 1 shows the time variations in the maxima of the upward and downward field-aligned current densities at the ionosphere height and the ionospheric plasma density. Here, t is the time after the quasi-steady state as shown in Ref. [2] (the system is in the quasi-steady state at $t = 0$). The enhancement of the ionospheric plasma density from $t \approx 3,700$ s to 3,800 s is observed. Then, the upward current drastically increases at around $t = 3,820$ s. This means that the ionospheric plasma density growth amplifies the field-aligned current by decreasing the ionospheric electric field. From the linear theory of M-I coupling, we obtain the response equation $\nabla_{\perp} \cdot E_{IS} = Z j_{\parallel}$ (Eq. (4) in Ref. [2]), where E_{IS} is the ionospheric electric field and Z is the magnetospheric impedance. Typically, Z is pure imaginary and $\text{Im}(Z)$ is positive (Ref. [2] and references therein). Thus, the phase lag of j_{\parallel} is a quarter of a period and the profile of j_{\parallel} takes the form of the derivative of the ionospheric electric field. Therefore, the field-aligned current is changed owing to the propagation of the ionospheric electric field variation into the magnetosphere. Furthermore, because the local decrease in the ionospheric electric field steepens the gradient of the ionospheric electric field around the decrease area, the upward current arises on one side of the decrease area and the return current appears on the other side. As the return current growth is not observed on the surface at around $t = 3,830$ s, this is probably attributed to some factors such as nonlinear processes, the system configuration [2], and the limit of the unstable region [2].

On the other hand, at around $t = 3,830$ s, the ionospheric plasma density intensively decreases while the upward current exhibits a sharp peak. This implies that the larger upward current does not necessarily induce the large growth rate of the ionospheric plasma density. In other

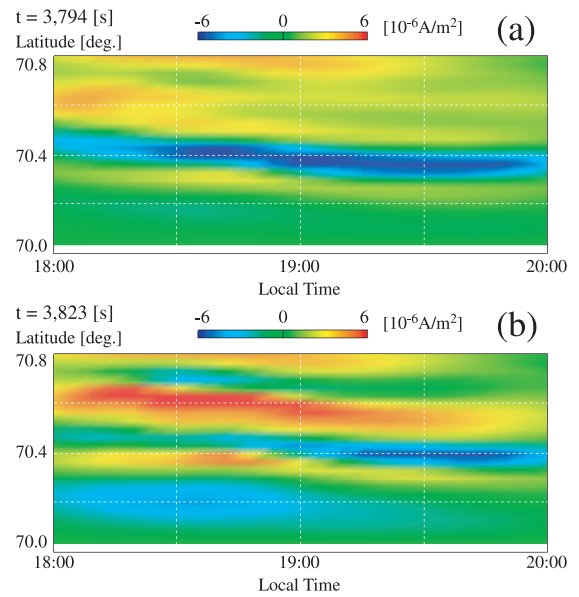


Fig. 2 Distributions of the field-aligned current density at the ionosphere height (a) at $t = 3,794$ s and (b) $t = 3,823$ s. The area that is shown in each panel lies from 18:00 to 20:00 local time and between 70.0° and 70.8° latitude.

words, the ionospheric plasma density growth due to accelerated electrons is not linearly proportional to the upward current. This feature arises from particle simulation which shows that the potential difference produced by current-driven (microscopic) instability is not proportional to the electron drift velocity v_d (i.e., the current) in the case of $v_d \gtrsim v_{Te}$ (Fig. 7 in Ref. [7]).

Furthermore, the ionospheric plasma density increases at around $t = 3,850$ s after the pulse of the upward current. Then, the second pulses of the upward and return currents occur at $t \approx 3,890$ s after the second high ionospheric plasma density state. The third ionospheric plasma density growth and the third pulses of the upward and return currents are shown between $t \approx 3,920$ s and 4,000 s in Fig. 1. The time interval between the pulses is about 90 s. This value is almost equal to τ_A . In other words, the characteristic time scale of the intermittent process is close to that of the macroscopic interaction between the magnetosphere and ionosphere. This means that the propagation of the ionospheric electric field variation into the magnetosphere, namely, the M-I coupling, plays an important role in the process.

Figures 2–4 show the distributions of the field-aligned current density at the ionosphere height at $t = 3,794$ s [Fig. 2 (a)], 3,823 s [Fig. 2 (b)], 3,867 s [Fig. 3 (a)], 3,896 s [Fig. 3 (b)], 3,955 s [Fig. 4 (a)], and 3,984 s [Fig. 4 (b)]. The panels (a) in these figures indicate the distribution before the first, second, and third pulses of the upward current. The panels (b) in these figures represent the distribution in the first, second, and third pulses of the upward current. By comparing the field-aligned current distribution

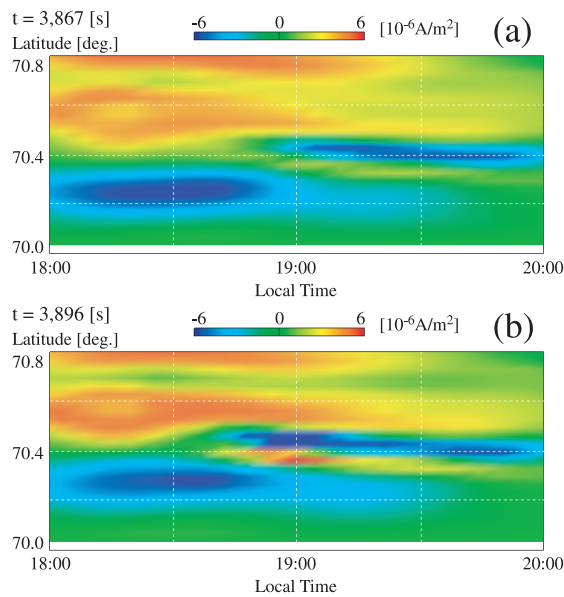


Fig. 3 Distributions of the field-aligned current density at the ionosphere height (a) at $t = 3,867$ s and (b) $t = 3,896$ s. The area that is shown in each panel lies on the same region as shown in Fig. 2.

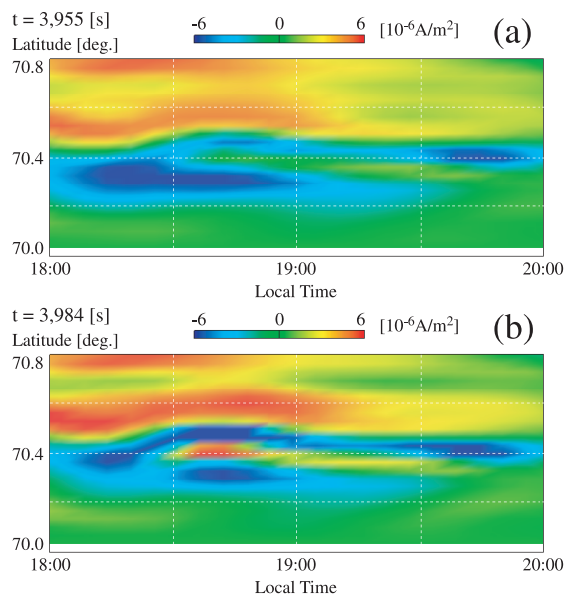


Fig. 4 Distributions of the field-aligned current density at the ionosphere height (a) at $t = 3,955$ s and (b) $t = 3,984$ s. The area that is shown in each panel lies on the same region as shown in Fig. 2.

before each pulse with that in each pulse, it is found that the positions of the upward current regions (i.e., auroral arcs) change around the sharp current growth. Figure 2 indicates

that the striped structure is shifted poleward by about 0.05° and an intensive upward current area appears around 19:00 local time and 70.55° latitude. Figure 3 shows that an intensive upward current area is formed around 19:00 local time and 70.35° latitude. Also, Fig. 4 reveals that an intensive upward current area is produced around 18:40 local time and 70.4° latitude. This fact and the pulsational property shown in Fig. 1 indicate that the microscopic process (i.e., the electron acceleration) provides drastic and intermittent transition to the macroscopic auroral arc structure.

4. Summary

Using the auroral MMI simulation code, we studied the process of quiet auroral arc formation, in particular, the response of the magnetosphere to the effect of auroral energetic electrons. We described the detailed investigations into some MMI simulation results of Ref. [4]. In the simulation, we observed the intermittent variations in the ionospheric plasma density and the field-aligned current. The characteristic time scale of these variations was estimated to be about the Alfvén transit time. Furthermore, drastic transitions in the auroral arc structure were found to occur with sharp growth in current. From these facts, the microscopic process (i.e., the electron acceleration) is believed to have a strong effect on the macroscopic auroral arc structure.

However, in this simulation, the magnetospheric data is so extensive that we have not been able to obtain sufficient temporal data to investigate the modes of the magnetospheric waves. This will be the topic of a future study.

Acknowledgments

This research has been performed mainly at the Institute for Research on Earth Evolution (IFREE) / JAMSTEC for which H. Hasegawa worked until April 2010. The authors would like to thank Dr. A. Kageyama, Dr. T. Sugiyama, Dr. K. Kusano, and Dr. S. Hirose for their valuable discussions. The simulation was performed on the original Earth Simulator / JAMSTEC. This work was supported in part by the NIFS Collaboration Research program (NIFS07KDAN001).

- [1] T. Sato, *J. Geophys. Res.* **83**, 1042 (1978).
- [2] H. Hasegawa, N. Ohno and T. Sato, *J. Geophys. Res.* **115**, A08304 (2010).
- [3] T. Sato, H. Takamaru and the Complexity Simulation Group, *Phys. Plasmas* **2**, 3609 (1995).
- [4] T. Sato, H. Hasegawa and N. Ohno, *Comput. Sci. Discovery* **2**, 015007 (2009).
- [5] T. Sato, *J. Phys.: Conf. Ser.* **16**, 310 (2005).
- [6] H. Takamaru *et al.*, *J. Phys. Soc. Jpn.* **66**, 3826 (1997).
- [7] H. Hasegawa and T. Sato, *Plasma Fusion Res.* **5**, 020 (2010).